Review Article

Pharmacokinetic Characteristics of Hydroxysafflor Yellow a in Normal and Diabetic Cardiomyopathy Mice

Yao R[1,2], Cao Y[2], Jiang R[1], Zhang X[1], Li F[1]* and Wang S[2]*

[1]Department of Traditional Chinese Medicine, The Air Force Medical University, China
[2]Department of Chinese Materia Medica and Natural Medicines, The Air Force Medical University, China

*Corresponding author: Siwang Wang, Department of Chinese Materia Medica and Natural Medicines, School of Pharmacy, The Air Force Medical University, Xi an 710032, Shanxi, China

Feng Li, Department of Traditional Chinese Medicine, The First Affiliated Hospital, The Air Force Medical University, Xi an 710032, Shanxi, China

Received: November 16, 2020; **Accepted:** December 16, 2020; **Published:** December 23, 2020

Abstract

Background: Hydroxysafflor Yellow A (HSYA), a major active water-soluble component in *Carthamus tinctorius* L., is considered a potential antioxidant with protective effects against myocardial injury. However, its pharmacokinetic characteristics in normal and Diabetic Cardiomyopathy (DCM) mice remain unknown. Thus, this study was designed to investigate the differences in the pharmacokinetics of HSYA between normal mice and streptozotocin-induced DCM mice.

Methods: HSYA in the mouse plasma was quantified using simple and efficient liquid chromatography-tandem mass spectrometry. The levels of oxidative stress-related cytokines were measured using appropriate kits.

Results: Compared with the normal group, the DCM group showed a significantly higher area under curve ($AUC_{(0-t)}$, $AUC_{(0-\infty)}$) value and peak plasma concentration, suggesting a higher uptake of HSYA in the DCM mice, and a significantly lower plasma clearance and apparent volume of distribution, suggesting slower elimination of HSYA in the DCM mice. Serum superoxide dismutase and glutathione peroxidase levels were significantly higher and malondialdehyde content was significantly lower in DCM mice than in normal mice, indicating the antioxidative stress effect of HSYA. Further correlation analysis showed that the serum HSYA content in the DCM mice showed a significant positive correlation with antioxidant enzyme levels.

Conclusion: These results showed that the pharmacokinetics of HSYA changed significantly in the DCM mice, which may improve the antioxidative stress effect of the drug.

Keywords: Hydroxysafflor yellow A; Pharmacokinetics; Diabetic cardiomyopathy; Liquid chromatography-tandem mass spectrometry

Abbreviations

AUC: Area Under the Curve; DCM: Diabetic Cardiomyopathy; DHE: Dihydroethidium; FBG: Fasting Blood Glucose; GSH-Px: Glutathione Peroxidase; HFD: High-Fat Diet; HSYA: Hydroxysafflor Yellow A; LVEF: Left Ventricular Ejection Fraction; LVFS: Left Ventricular Fractional Shorting; MDA: Malondialdehyde; QC: Quality Control; ROS: Reactive Oxygen Species; RSD: Relative Standard Deviation; SOD: Superoxide Dismutase; STZ: Streptozotocin

Introduction

The International Diabetes Federation has reported that approximately 463 million adults worldwide had diabetes in 2019 and estimated that this number will reach 700 million in 2045 [1]. Diabetes has been a global public health problem. Diabetic Cardiomyopathy (DCM) is a major complication of diabetes. Chronic diabetes can induce specific cardiomyopathy and eventually heart failure, which is the main cause of disability and death in patients with diabetes [2]. Oxidative stress and free radicals are the primary or auxiliary factors involved in DCM [3]. Diabetes with hyperglycemia and/or hyperlipidemia is associated with an increase in the production of free radicals or impairment of antioxidant defense capabilities. Nutritional drugs and functional foods with antioxidant activities can maintain the balance between oxygen free radicals and antioxidant enzymes, thereby preventing DCM. *Carthamus tinctorius* L, as a medicinal and food homologous herb, is considered an excellent antioxidant [4,5]. It exhibits protective effects in myocardial injury [6] and hypoglycemic effects [7,8] and improves microcirculation [9]. In traditional Chinese medicine, safflower is a major decoction; water-soluble components play an important role in its curative effect. Phytochemical research shows that the major component in safflower water-soluble extract is safflor yellow [10]. Among these compounds, the content of Hydroxysafflor Yellow A (HSYA), (Figure 1) is the highest, and it has been used as the Quality Control (QC) marker for safflower in the Chinese Pharmacopoeia [11]. The content of HSYA is related to its antioxidant capacity. In recent years, most pharmacokinetic studies on HSYA have administered the drug intravenously [12-14]. However, in traditional Chinese medicine treatment, safflower extract is not a pure biologically active ingredient but is taken orally as a decoction. In addition, the effect of DCM on the pharmacokinetics of HSYA has not been reported. Under pathological conditions, changes in the expression of metabolic enzymes, transporters, and genes related to drug metabolism and transport in the body may affect pharmacokinetics. In long-term diabetes, the blood vessels, heart, and kidneys may generate organic lesions, which further affect body functions and change the pharmacokinetics of HSYA.
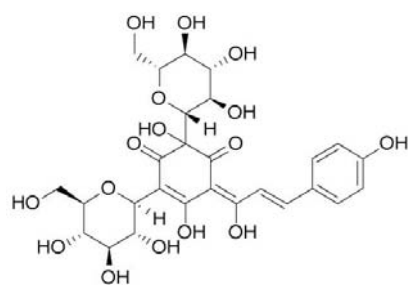
Figure 1: Chemical structures of hydroxysafflor yellow A.

Therefore, in this study, we investigated the differences in the pharmacokinetics of HSYA between normal and DCM mice following gavage administration of HSYA solution and determined the effect of HSYA on Superoxide Dismutase (SOD) and Glutathione Peroxidase (GSH-Px) activities. The correlation between the pharmacokinetics and pharmacodynamics of HSYA in DCM mice could provide a basis for the clinical treatment of diabetic cardiomyopathy.

Methods

Materials and reagents

HSYA exhibiting 98.0 % purity was obtained from Shanghai Yuanye (Shanghai, China); isorhamnetin-3-O-neohesperidoside (99.0 % purity), used as the Internal Standard (IS), was obtained from the Shengzhong Chemical Reagent, Co., Ltd. (Shanghai, China); high-fat (45 FDC) purified rodent diet (HFD) was purchased from Dytz Biotechnology (Wuxi, China); Streptozotocin (STZ) was purchased from Sigma-Aldrich (USA); methanol (HPLC grade) was provided by Honeywell Burdick and Jackson (SK Chemicals, Korea); and Methanoic acid (HPLC grade) was purchased from Alighting Biochemical Technology (Shanghai, China). Ultrapure water was prepared using the Direct-Q® microporous water purification system from Merck Millipore GMBH.

Animals

C57BL/6 mice (male, 23±2 g) were provided by the animal experimental center of the Air Force Medical University (Xi an, China). The animals were provided free access to food and water and maintained at 22±2 °C, 50±10 % humidity. All protocols used in this study were approved by the Ethics Committee for Animal Experimentation of the Air Force Medical University (approval No: IACUC-20170509) and performed according to the National Institute of Health Guide for the Care and Use of Laboratory Animals (NIH Publications No. 80-23) revised in 1996.

Induction of diabetic cardiomyopathy

After comparing different doses of STZ and times of administration, our research group had previously established a C57BL/6 DCM mouse model with stable blood glucose level and low mortality. The detailed method is as follows [15]: the mice were fed HFD for 4 weeks and then intraperitoneally injected with STZ at a dose of 60 mg/kg (dissolved in citrate buffer, pH=4.5) for 3 days. The mice in the normal group were injected with the same volume of citrate buffer. After 2 weeks, the Fasting Blood Glucose (FBG) was monitored using Bayer's BREEZE 2 meter (Bayer Health Care LLC, Mishawaka, USA), and FBG >11.1mm was considered to indicate

diabetes. The diabetic mice were continued to be fed the HFD. After 12 weeks, echocardiography revealed left ventricular diastolic dysfunction, suggesting the establishment of a DCM mouse model.

Determination of cardiac function

Mice were anesthetized by 1.0 % isoflurane to maintain heart rates at 400–500 beats/min and cardiac functions were determined using transthoracic echocardiography with a Visual-Sonics Vevo 770 ultrasound system (Toronto, Canada). Left Ventricular Fractional Shorting (LVFS), Left Ventricular Ejection Fraction (LVEF), left ventricular end-diastolic volumes, and left ventricular end-systolic volumes were determined using computer algorithms.

Hematoxylin-Eosin (HE) and Masson's trichrome staining

The heart samples were collected, fixed in 4% paraformaldehyde, dehydrated in a gradient series of alcohol, treated with xylene, embedded in paraffin, and cut into 5-μm thick sections. The paraffin sections were stained with conventional HE to observe the morphological and structural changes in the myocardium and blood vessels. Masson staining was performed to observe the degree of fibrosis around the myocardium and blood vessels. After staining, the sections were observed and photographed using a Nikon ECLIPSE 80i optical microscope.

Reactive Oxygen Species (ROS) detection

ROS in myocardial frozen sections was detected by Dihydroethidium (DHE) staining, as previously reported [16,17]. After being stained with DHE and 4′, 6-diamidino-2-phenylindole, the tissue sections were observed using a laser confocal microscope (Olympus FV1000, Olympus, Japan). The fluorescence density value was determined using Image-Pro Plus (Version 6.0, Media Cybernetics, USA).

Assay of serum biochemical indexes related to oxidative stress

Relative levels of GSH-Px, SOD and Malondialdehyde (MDA) were all purchased from Nanjing Jiancheng Bioengineering Institute in China and determined using enzyme-linked immunosorbent assay kits, and the procedures were performed as per the manufacturer's protocol.

Instrumentation and conditions

The QC samples and the real plasma samples were analyzed by a Liquid Chromatography/Mass Spectrometry (LC/MS) system consisting of a Thermo Scientific Dionex Ultimate 3000 HPLC system coupled to a TSQ Quantum Ultratriple tandem quadruple mass spectrometer equipped with an electrospray ionization source. Chromatographic separation was achieved on a Welch Ultimate XB-C18 column (150×4.6 mm, 3μm). The mobile phase consisted of 0.1% formic acid solution (A) and methanol (B) at 1.2mL/min with a gradient as follows: 0.00-1.50 min, 20% B; 1.51-4.20 min, 95% B; 4.21-5.50 min, 20% B. The MS was operated as follows: ion source, electrospray ion; monitoring mode: positive selected ion; spray voltage, 4000 V; capillary temperature, 350°C. Ions exhibiting m/z 613.12 and 627.20 were selected as the parent ions, and those with m/z 211.02 and 302.79 were selected as the daughter ions for HSYA and IS.
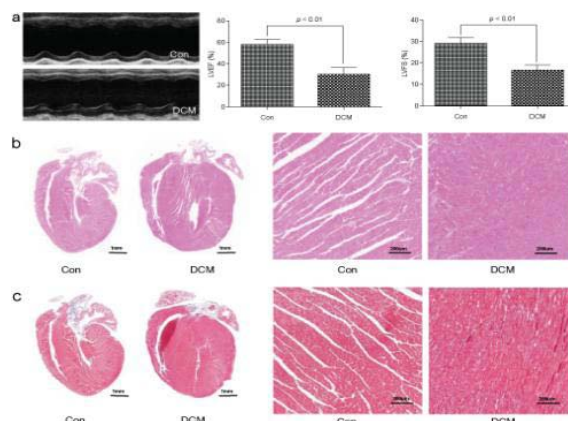
Figure 2: Cardiac function and pathology in diabetic cardiomyopathy mice.
A: Echocardiography and cardiac function of Left Ventricular Ejection Fraction (LVEF) and Left Ventricular Fractional Shorting (LVFS); the values are expressed as the mean ± Standard Deviation (SD), $^{**}P < 0.01$ *vs* Control (Con).
B: Representative images for HE staining of the heart tissues.
C: Representative images for Masson's trichrome staining of the heart tissues.

Table 1: Precision and recovery of HSYA in mouse plasma (n=8).

Prepared concentration	Intra-day		Inter-day		Average recovery
($\mu g \cdot mL^{-1}$)	Measured concentration ($\mu g \cdot mL^{-1}$)	Precision (RSD%)	Measured concentration ($\mu g \cdot mL^{-1}$)	Precision (RSD%)	(%)
0.02	0.0208	3.2	0.0198	8.2	101.5
1	0.9485	9.5	0.8958	6.5	92.22
10	11.5205	4.1	10.2521	5.8	108.86

Table 2: The stability of HSYA in mouse plasma (n=8).

Prepared concentration	Room temperature for 2 h		Refrigerator at -80 °C		Three freeze-thaw cycles	
($\mu g \cdot mL^{-1}$)	Measured concentration	RSD (%)	Measured concentration	RSD (%)	Measured concentration	RSD (%)
0.02	0.0185	11.2	0.0188	5.1	1.86	5.9
1	1.0323	6.2	1.0624	4.2	105.44	2.6
10	10.5888	7.8	10.6211	10.2	1040.98	6.4

Preparation of standards, plasma samples, and quality control samples

The HSYA standard was prepared as a stock solution of 5.00mg/mL with methanol as a solvent. A stock solution of 2.00mg/mL isorhamnetin-3-O-neohesperidin standard was prepared as the IS and subsequently diluted to 1μg/mL to obtain the working solution. We accurately aspirated 50μL of the plasma sample, added 150μL of methanol, and centrifuged the sample at 13680g for 10 min. Subsequently, 150μL of the supernatant was collected, and 10μL of the IS solution was added. The supernatant was then centrifuged at 13680g for 10 min to obtain the plasma samples.

The HSYA stock solution was diluted with methanol; the IS solution was added to it to prepare a series of standard plasma solutions at concentrations of 0.01, 0.1, 0.5, 1, 5, and 10 μg/mL. High, medium, and low concentration QC samples were 0.02, 1.00 and 10 μg/mL.

Pharmacokinetic analysis

For the pharmacokinetic study, mice were randomly assigned to two groups: normal (normal, n=80) and DCM groups (DCM, n=100). First, the DCM group was administered STZ$^+$HFD to induce DCM. Subsequently, both the normal and DCM groups were orally administered 60mg/kg HSYA, following which blood samples were collected *via* intracardiac puncture into heparinized tubes at 0, 5, 10, 20, 30, 45, 60, 90, 120, 240 and 480 min. The plasma samples were separated immediately by centrifugation at 4°C and 4000rpm for 15 min and subsequently stored at -80°C for further analysis.

Statistical analysis

Pharmacokinetic parameters were analyzed using the Drug and Statistics software (DAS; version 2.1.1). The GraphPad Prism 5.01 software was used for data statistical processing, and the data are presented as the mean±SD. One-way ANOVA was used to compare the differences between groups, with $P < 0.05$ indicating a statistically significant difference.

Results and Discussion

Pathological and functional changes in DCM mouse model

DCM is a secondary cardiomyopathy. Long-term hyperglycemia and hyperlipidemia eventually lead to cardiac dysfunction [18], including left ventricular hypertrophy, left ventricular diastolic dysfunction, and systolic dysfunction. Clinically, cardiac dysfunction in patients with DCM mainly manifests as changes in the ejection

Table 3: Pharmacokinetic parameters of HSYA in mice after oral administration of HSYA (n=8).

Pharmacokinetic parameters	Units	Normal group	DCM group
		Mean ± SD	Mean ± SD
C_{max}	$\mu g \cdot mL^{-1}$	2.41±0.23	4.08±0.51**
T_{max}	h	0.78±0.07	1.02±0.08
$t_{1/2}$	h	1.54±0.12	2.00±0.09
$MRT_{(0-t)}$	h	0.82±0.34	1.08±0.24
$AUC_{(0-t)}$	$\mu g \cdot h \cdot mL^{-1}$	5.07±0.58	11.74±0.55**
$AUC_{(0-\infty)}$	$\mu g \cdot h \cdot mL^{-1}$	5.21±0.56	13.27±0.62**
CL	$mL \cdot (h \cdot kg)^{-1}$	4.58±0.55	1.70±0.18**
V_d	$L \cdot kg^{-1}$	6.21±0.87	3.28±0.75**

Table 4: The fitting equations for MDA, SOD, and GSH-Px in mouse plasma.

	The fitting equation	R
SOD	y=29.26 lnx+180.3	0.75
MDA	y=-1.05 lnx+20.60	0.77
GSH-Px	y=26.60 lnx+188.4	0.82

fraction and peak filling rate according to echocardiography and radionuclide imaging. Metabolic disorders in patients with type 2 diabetes can cause extensive myocardial damage, manifested as cardiomyocyte hypertrophy, degeneration, and focal necrosis [19,20]. Several studies have reported the establishment of a DCM model through the administration of a continuous high-fat diet combined with intraperitoneally injected STZ [21-23]; the difference in the STZ dose and number of injections is the key to model preparation. We established a DCM mouse model by HFD feeding with three intraperitoneal injections of STZ (60mg/kg). In our study, the DCM group exhibited significantly lower values for LVEF and LVFS than the normal group (*P* <0.01), based on ultrasonography. The HE staining results showed hypertrophy and a disordered arrangement of cardiomyocytes, with the proliferation of a large number of cardiac fibroblasts and high levels of inflammatory cell infiltration. Masson staining showed a significant increase in collagen fiber synthesis in the myocardium and perivascular tissue (Figure 2). These results are consistent with the changes in cardiac function and cardiomyocytes in DCM.

LC-MS method validation

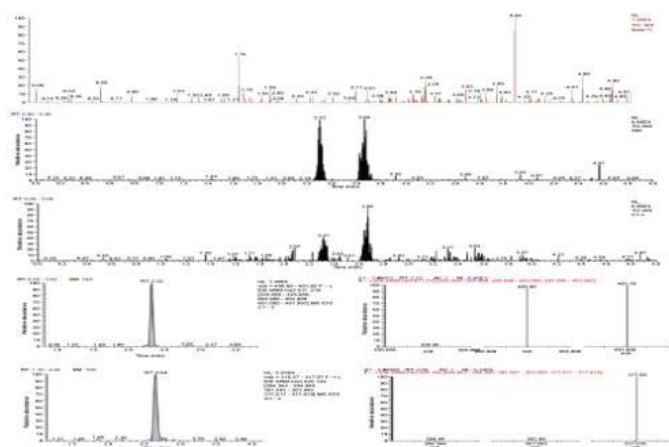The detection of HSYA and IS by SIM mode was highly selective with no interference (Figure 3). Presents the representative chromatograms of the total ion flow for the blank plasma samples, blank plasma samples spiked with HSYA and IS, and plasma samples after oral administration of HSYA. It also depicts the extract ion flow diagrams for HSYA and IS in mice after the oral administration of HSYA. HSYA exhibited satisfactory linearity with the regression equation of y=-272.641+ 34.4469 x and linear range of 0.01-10 μg/mL. The intra- and inter-day precision and recovery of the HSYA from the validation of this method were acceptable (Table 1). The Relative Standard Deviation (RSD) of intra-day and inter-day precisions was less than 15%, and the relative recovery rate in the plasma was between 92.22-101.50 %. Stability investigation showed that the RSD values of the samples were less than 15% after the samples were placed at room temperature (25°C) for 2 h, frozen for 45 days at -80°C, and subjected to a freeze-thaw cycle for three times, which met the LC-MS/MS requirements for biological samples (Table 2).

Pharmacokinetic studies

Long-term hyperglycemia induces changes in the activity of metabolic enzymes and transport proteins related to drug absorption and metabolism and in gene expression *in vivo*. Moreover, long-term diabetes can lead to pathological changes in the heart, kidney, and blood vessels that affect organ or whole-body functions, which could further change the pharmacokinetic behavior of drugs [24-26]. To the best of our knowledge, this is the first study to demonstrate the pharmacokinetic characteristics of HSYA in DCM mice. The mean plasma concentration-time profiles are presented in (Figure 4). The major pharmacokinetic parameters of HSYA, as calculated using the non-interventricular model, are presented in (Table 3).

Figure 3: Selected ion monitoring chromatograms. Selected ion monitoring chromatograms representing.
A: total ion flow for the plasma from the control mice.
B: total ion flow for the control mouse plasma spiked with HSYA and IS.
C: total ion flow for plasma samples after oral administration of HSYA.
D: extract ion flow diagrams for HSYA.
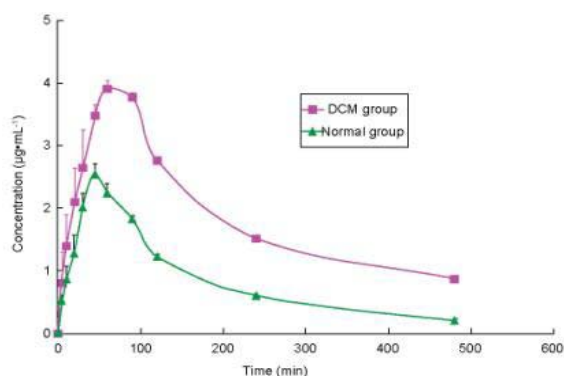**E:** extract ion flow diagrams for IS.

Figure 4: The mean plasma concentration-time profiles of HSYA in normal and diabetic cardiomyopathy mice.
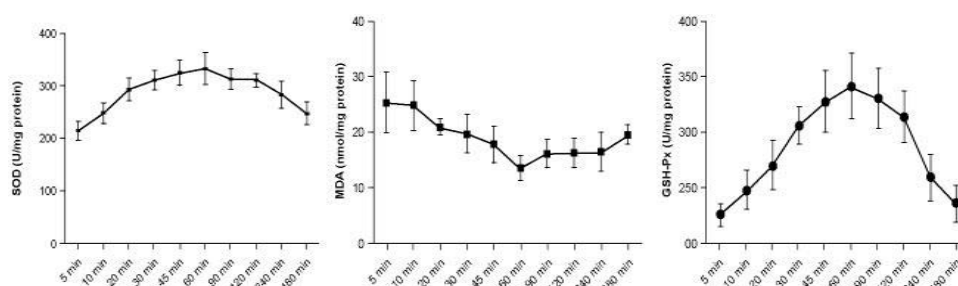

Figure 5: Plasma concentration of SOD, MDA, and GSH-Px changes with time after HSYA administration in DCM mice.
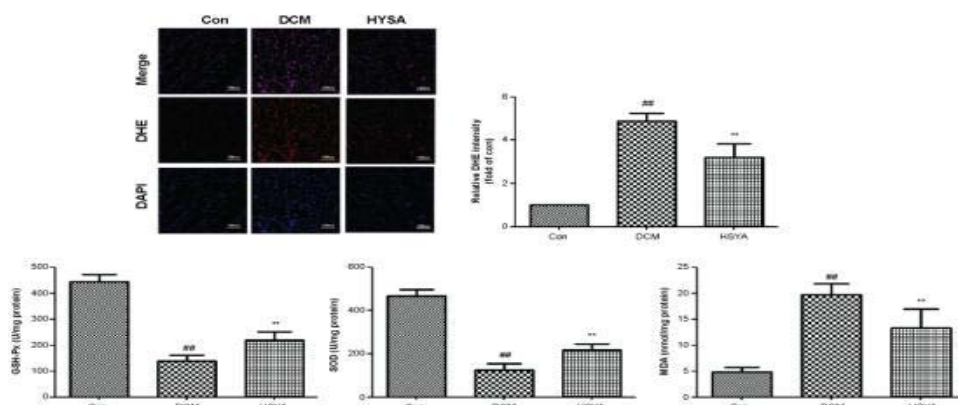

Figure 6: Effects of HSYA on oxidative stress in DCM mice.
A: Representative images of Dihydroethidium (DHE) staining and the DHE intensity.
B: Malondialdehyde (MDA) levels in myocardial tissues.
C: Superoxide Dismutase (SOD) activity in myocardial tissues.
D: Glutathione Peroxidase (GSH-Px) activity in myocardial tissues. Values are showed as mean ± standard deviation (SD). $^{##}P$ <0.01 *vs* Control (Con) group, $^{**}P$ < 0.01 *vs* DCM group.

Compared with the normal group, the DCM mice exhibited a significantly higher area under the curve ($AUC_{(0-t)}$, $AUC_{(0-\infty)}$) and peak plasma concentration for HSYA ($P<0.01$), which suggested a high uptake in DCM mice; furthermore, the plasma clearance and apparent volume of distribution ($P<0.01$) were significantly lower in the DCM mice, which indicated that the elimination was slower than that in the normal group.

Antioxidant stress effect

Numerous studies have shown that oxidative stress induced by hyperglycemia is the major risk factor for DCM [27,28]. Oxidative stress promotes myocardial injury, which is caused by the imbalance between excessive ROS and endogenous ROS scavenging antioxidant systems [29,30]. ROS and unsaturated fatty acids form lipid peroxides, and the MDA content reflects the damage degree of oxidative stress [31,32]. Furthermore, a reduction in endogenous antioxidant capacity leads to oxidative stress in the pathogenesis of DCM. SOD and GSH-Px are two important indexes that reflect the antioxidant defense ability. SOD is the most important substance in the free radical scavenging system; it can convert superoxide anion radicals to
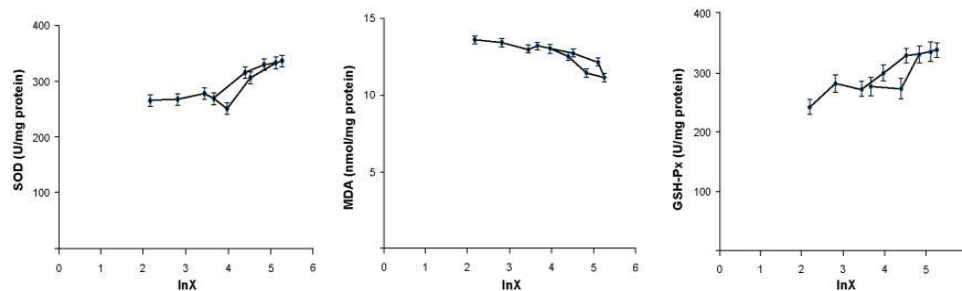
Figure 7: The correlation between the content of Hydroxysafflor Yellow A (HSYA) and antioxidative stress effect.

H_2O_2. This superoxide-anion scavenging activity of SOD reflects the intracellular antioxidant capacity [29,33]. GSH-Px removes excess ROS by catalyzing the breakdown of H_2O_2 and lipid peroxidation, thereby protecting the myocardial tissue from oxidative stress [29,34].

In our study, the levels of ROS in heart tissue were detected by DHE staining. As presented in (Figure 5), DHE fluorescence intensity in the DCM group was significantly higher than that in the normal group ($P<0.01$). Nevertheless, the level of oxidative stress was higher in the DCM group, which manifested as an increase in plasma MDA content and a decrease in SOD and GSH-Px activity ($P<0.01$). These results suggest that oxidative stress is enhanced in the DCM mice, which is consistent with previous reports [30,31,33]. After the oral administration of the HSYA solution for 1 h, the fluorescence intensity of DHE in the mouse heart tissue was significantly reduced ($P <0.01$), indicating a decrease in ROS production *in vivo*. The activity of GSH-Px and SOD in the plasma of the DCM mice was significantly decreased ($P <0.051$), and the content of MDA was significantly increased ($P<0.01$); (Figure 6). The results indicated that HSYA exerted a protective effect on the myocardium against oxidative damage in DCM. Subsequently, we analyzed the levels of SOD, GSH-Px and MDA in the mouse plasma at different time points after HSYA was administered by gavage. As the levels of SOD, GSH-Px, and MDA in the normal group did not change significantly over time, no statistical analyses were performed. As presented in (Figure 5), SOD and GSH-Px activities in the plasma of the DCM mouse increased first and then decreased, whereas the MDA content decreased first and subsequently increased. The results suggest that there is a time–effect change in the plasma HSYA content and antioxidant capacity.

To further explore the relationship between the plasma HSYA content and the antioxidative stress effect, the logarithm of the HSYA concentration (X) in the plasma was plotted as the abscissa, and the levels of GSH-Px, SOD, and MDA were plotted as the ordinate. The dose-effect relationship was analyzed by the scattered-point correlation method, and $Y=a+b \cdot \ln X$ was used for mathematical fitting. The plasma concentration of HSYA correlated with the levels of GSH-Px, SOD activity, and MDA, suggesting a positive correlation between the concentration of HSYA in plasma and the antioxidant capacity in DCM mice (Figure 7 & Table 4).

Conclusion

In summary, our results suggest that the pharmacokinetics of HSYA can be altered in the DCM mice. More importantly, the HSYA level in the plasma correlated with the antioxidant capacity, which indicates the pharmacokinetic rationale for the potential use of HSYA

for treating DCM. However, as diabetic cardiomyopathy is a chronic disease, the pharmacokinetics of multiple-dose administration of HSYA need to be further studied.

Declarations

Ethics approval and consent to participate: All protocols used in this study were approved by the Ethics Committee for Animal Experimentation of the Air Force Medical University and performed according to the National Institute of Health Guide for the Care and Use of Laboratory Animals (NIH Publications No. 80-23) revised in 1996. Consent to participate is not applicable.

References

1. International Diabetes Federation (IDF). Diabetes Atlas: 9th Edition. International Diabetes Federation; 2019.

2. Trachanas K, Sideris S, Aggeli C Poulidakis E, Gatzoulis K, Tousoulis D, et al. Diabetic cardiomyopathy: From pathophysiology to treatment. Hellenic J Cardiol. 2014; 55: 411-421.

3. Palomer X, Pizarro-Delgado J, Vazquez-Carrera M. Emerging actors in diabetic cardiomyopathy: heartbreaker biomarkers or therapeutic targets? Trends Pharmacol Sci. 2018; 39: 452-467.

4. Choi EM, Kim GH, Lee YS. *Carthamus tinctorius* flower extract prevents H_2O_2-induced dysfunction and oxidative damage in osteoblastic MC3T3-E1 cells. Phytother Res. 2010; 24: 1037-1041.

5. Han SY, Li HX, Bai CC, Wang L, Tu PF. Component analysis and free radical-scavenging potential of Panax notoginseng and *Carthamus tinctorius* extracts. Chem Biodivers. 2010; 7: 383-391.

6. Delshad E, Yousefi M, Sasannezhad P, Rakhshandeh H, Ayati Z. Medical uses of *Carthamus tinctorius* L. (Safflower): A comprehensive review from traditional medicine to modern medicine. Electron Physician. 2018;10: 6672-6681.

7. Asgary S, Rahimi P, Mahzouni P, Madani H. Antidiabetic effect of hydroalcoholic extract of *Carthamus tinctorius* L. in alloxan-induced diabetic rats. J Res Med Sci. 2012; 17: 386-392.

8. Lee M, Li H, Zhao H, Suo M, Liu D. Effects of hydroxysafflor yellow A on the PI3K/AKT pathway and apoptosis of pancreatic β-cells in type 2 diabetes mellitus rats. Diabetes Metab Syndr Obes. 2020; 13: 1097-1107.

9. Liang XT. Basic Study of Common Chinese Medicine Part II. Beijing: Science Press; 2004: 102-115.

10. Asgarpanah J, Kazemivash N. Phytochemistry, pharmacology and medicinal properties of *Carthamus tinctorius* L. Chin J Integr Med. 2013; 19: 153-159.

11. The State Pharmacopoeia Commission of China. Pharmacopoeia of the People's Republic of China, Part I. Beijing: Chemical Industry Press. 2015: 10.

12. Chu D, Liu W, Huang Z, Liu S, Fu X, Liu K. Pharmacokinetics and excretion of hydroxysafflor yellow A, a potent neuroprotective agent from safflower, in rats and dogs. Planta Med. 2006; 72: 418-423.

13. Zhang HF, Guo JX, Huang LS, Ping QN. Pharmacokinetics of hydroxysafflor yellow A in rats. J ChinaPharm Univ. 2006; 37: 456-460.

14. Zhan Y, Xu JP, Liang JB, Sheng LS, Xiang BR, Zou QG, et al. Simultaneous LC-MS-MS analysis of Danshensu, salvianolic acid B, and hydroxysafflor yellow A in beagle dog plasma, and application of the method to a pharmacokinetic study of Danhong lyophilized powder for injection. Chromatographia. 2008; 68: 71-79.

15. Li K, Zhai M, Jiang L, Song F, Zhang B, Li J, et al. Tetrahydrocurcumin ameliorates diabetic cardiomyopathy by attenuating high glucose-induced oxidative stress and fibrosis *via* activating the SIRT1 pathway. Oxid Med Cell Longev. 2019; 2019: 6746907.

16. Zhang B, Zhai M, Li B, Liu Z, Li K, Jiang L, et al. Honokiol ameliorates myocardial ischemia/reperfusion injury in Type 1 diabetic rats by reducing oxidative stress and apoptosis through activating the SIRT1-Nrf2 signaling pathway. Oxid Med Cell Longev. 2018; 2018: 3159801.

17. Zhai M, Liu Z, Zhang B, Jing L, Li B, Li K, et al. Melatonin protects against the pathological cardiac hypertrophy induced by transverse aortic constriction through activating PGC-1β: *in vivo* and *in vitro* studies. J Pineal Res. 2017; 63: e12433.

18. Fernandez EB. Glucolipotoxicity, resistance to the action of insulin and type 2 diabetes mellitus. An R Acad Nac Med (Madr). 2007; 124: 547-557.

19. Aneja A, Tang WH, Bansilal S, Garcia MJ, Farkouh ME. Diabetic cardiomyopathy: Insights into pathogenesis, diagnostic challenges, and therapeutic options. Am J Med. 2008; 121: 748-757.

20. Marwick TH, Ritchie R, Shaw JE, Kaye D. Implications of underlying mechanisms for the recognition and management of diabetic cardiomyopathy. J Am Coll Cardiol. 2018; 71: 339-351.

21. Cheng Y, Wang S, Zheng Y. GW26-e4479 Nrf2 is crucially required for sulforaphane to prevent high fat diet/low dose STZ induced diabetic cardiomyopathy. J Am Coll Cardiol. 2015; 66: C37.

22. Tang S, Liu X, Ye JM, Hu TT, Yang YY, Han Y, et al. Isosteviol ameliorates diabetic cardiomyopathy in rats by inhibiting ERK and NFB signaling pathways. J Endocrinol. 2018; 238: 47-60.

23. Abdel-Hamid AAM, Firgany AEL. Atorvastatin alleviates experimental diabetic cardiomyopathy by suppressing apoptosis and oxidative stress. J Mol Histol. 2015; 46: 337-345.

24. Lam JL, Jiang Y, Zhang T, Zhang EY, Smith BJ. Expression and functional analysis of hepatic cytochromes P450, nuclear receptors, and membrane transporters in 10- and 25-week-old db/db mice. Drug Metab Dispos. 2010; 38: 2252-2258.

25. Gravel S, Panzini B, Belanger F, Turgeon J, Michaud V. A pilot study towards the impact of type 2 diabetes on the expression and activities of drug metabolizing enzymes and transporters in human duodenum. Int J Mol Sci. 2019; 20: 3257.

26. Posch M, Tillner J, Huser A, Teichert L, Einig C, Bergmann K, et al. Safety, pharmacokinetics, and pharmacodynamics of the novel dual GLP-1/glucagon agonist SAR425899 in healthy subjects and diabetes patients. American Diabetes Association. 2016: 65.

27. Wang XT, Gong Y, Zhou B, Yang JJ, Cheng Y, Zhao JG, et al. Ursolic acid ameliorates oxidative stress, inflammation and fibrosis in diabetic cardiomyopathy rats. Biomed Pharmacother. 2018; 97: 1461-1467.

28. Varga ZV, Giricz Z, Liaudet L, Hasko G, Ferdinandy P, Pacher P. Interplay of oxidative, nitrosative/nitrative stress, inflammation, cell death and autophagy in diabetic cardiomyopathy. Biochim Biophys Acta. 2015; 1852: 232-242.

29. Aliciguzel Y, Ozen I, Aslan M, Karayalcin U. Activities of xanthine oxidoreductase and antioxidant enzymes in different tissues of diabetic rats. J Lab Clin Med. 2003; 142: 172-177.

30. Liang D, Zhong P, Hu J, Lin F, Qian Y, Xu Z, et al. EGFR inhibition protects the cardiac remodeling through attenuating oxidative stress in STZ-induced diabetic mouse model. J Mol Cell Cardiol. 2015; 82: 63-74.

31. Ye G, Metreveli SN, Donthi RV, Xia S, Xu M, Carlson EC, et al. Catalase protects cardiomyocyte function in models of type 1 and type 2 diabetes. Diabetes. 2004; 53: 1336-1343.

32. Traverso N, Menini S, Odetti P, Pronzato MA, Cottalasso D, Marinari UM. Lipoperoxidation in hepatic subcellular compartments of diabetic rats. Free Radic Biol Med. 1999; 26: 538-547.

33. Shen X, Zheng S, Metreveli NS, Epstein PN. Protection of cardiac mitochondria by overexpression of MnSOD reduces diabetic cardiomyopathy. Diabetes. 2006; 55: 798-805.

34. Bastar I, Seckin S, Uysal M, Aykac-Toker G. Effect of streptozotocin on glutathione and lipid peroxide levels in various tissues of rats. Res Commun Mol Pathol Pharmacol. 1998; 102: 265-272.